

## RESEARCH ON THE APPLICATION OF LASER CAMERA TO SUPPORT LVDT IN GEOTECHNICAL LABORATORY WORK

Nguyễn Ngọc Thuyết<sup>1</sup>, Nguyễn Thị Ngân<sup>2</sup>

<sup>1, 2</sup> Viện Khoa học công nghệ xây dựng

Email: <sup>1</sup> thuyetibst@gmail.com, <sup>2</sup> thanhngan\_hp@yahoo.com

DOI: <https://doi.org/10.59382/pro.intl.con-ibst.2023.ses3-18>

**TÓM TẮT:** Các thử nghiệm trong phòng thí nghiệm là cần thiết để phân tích hành vi của các mô hình và vật liệu địa kỹ thuật. Hai trong những phương pháp phổ biến nhất để đo độ dịch chuyển trong các thử nghiệm trong phòng thí nghiệm là đồng hồ so và máy biến áp vi sai biến tuyến tính (LVDT). Tuy nhiên, việc sử dụng những thiết bị này có một số hạn chế như chỉ đo được các điểm rời rạc và với đồng hồ so thì bề mặt cần đo phải có độ cứng nhất định. Đặc điểm này là một hạn chế lớn bởi vì vật liệu địa chất thường không phải là một khối cứng nhắc. Để khắc phục những hạn chế này, các tác giả đã nghiên cứu sử dụng máy ảnh laser như một giải pháp hỗ trợ cho LVDT và đồng hồ so. Máy ảnh laser cung cấp tỷ lệ lấy mẫu cao, tuy nhiên, độ chính xác của chúng thì cần khảo sát một cách kỹ lưỡng khi mà hiện nay chúng chủ yếu được ứng dụng để đo khoảng cách lớn. Bài báo này trình bày cách khảo sát độ chính xác của máy ảnh laser bằng những quan sát trực quan, tin cậy, xem xét các nghiên cứu gần đây về việc sử dụng máy ảnh laser trong các thử nghiệm trong phòng thí nghiệm, bao gồm các ưu điểm, hạn chế và ứng dụng tiềm năng của chúng từ đó đánh giá được tiềm năng áp dụng máy ảnh laser để đo khoảng cách thay cho LVDT. Chúng tôi cũng thảo luận về những thách thức và hướng đi trong tương lai của việc sử dụng máy ảnh laser trong thử nghiệm trong phòng thí nghiệm. Nhìn chung, việc sử dụng máy ảnh laser có khả năng cải thiện độ chính xác và hiệu quả của các thử nghiệm trong phòng thí nghiệm và có thể trở thành một phương pháp hiệu quả để đo chuyển vị trong tương lai.

**TỪ KHÓA:** đầu đo LVDT, Máy ảnh laser, thí nghiệm mô hình.

*ABSTRACTS: Laboratory tests are essential for analyzing the behavior of geotechnical materials and models. Two of the most common methods for measuring displacement in laboratory tests are Dial indicator and Linear variable differential transformer (LVDT). However, using these equipments has some limitations, such as measuring only discrete points, and Dial indicators require surfaces to be measured must have a certain hardness. This feature is a significant limitation because geomaterials are not usually rigid masses. To overcome these limitations, the authors studied using laser cameras to support the LVDTs and the Dial indicators. Laser cameras offer high sampling rates, but their accuracy needs to be carefully investigated as they are mainly used to measure large distances. In this paper, we show how to investigate the accuracy of laser cameras with reliable, intuitive observations, reviewing recent studies on using laser cameras in laboratory tests. Experiments, including their advantages, limitations and potential applications: The potential application of laser cameras to measure distances can be evaluated instead of LVDT. We also discuss the challenges and future directions of using laser cameras in laboratory testing. The results showed that laser cameras could improve the accuracy and efficiency of laboratory tests and may become a preferred method for displacement measurement in the future.*

**KEYWORDS:** LVDT, Laser camera, model tests.

## 1. INTRODUCTION

The standard displacement measuring devices in today's common types of experiments are the LVDT and the dial indicator. These devices have been used for a long time and have proven effective. However, in actual use, they also reveal certain limitations. Some of their significant disadvantages when applied in geotechnical experiments are described below.

### 1.1. Dial indicator

A Dial indicators is a device that works according to the mechanical principle with a point-measuring head (Figure 1). For the measuring head to move, the contact position must have a specific stiffness so that the force can be transferred to the gauge head. This feature makes it imprecise to directly measure the displacement of soft soil surfaces in geotechnical experiments. The fact is that this type of device is rarely used for direct measurement of soil surfaces, but gauge heads are often arranged in contact with hard surfaces such as concrete or metal.

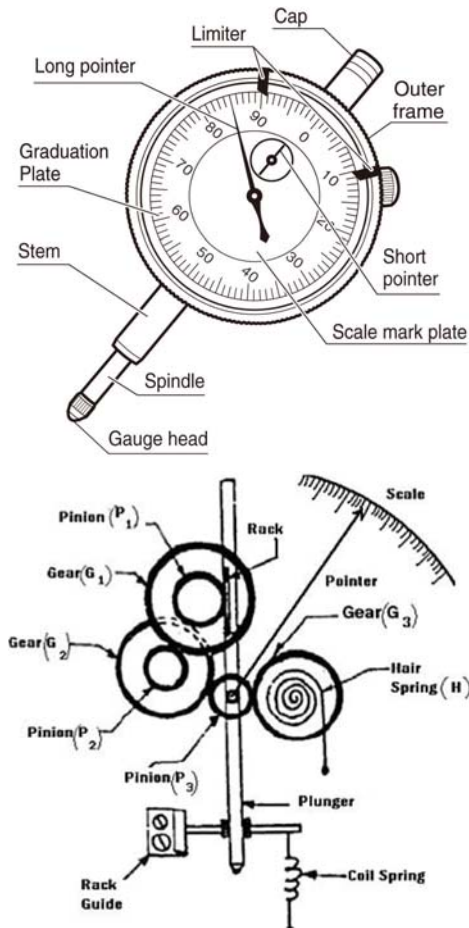


Figure 1. Principle and parts of Dial indicators [1]

### 1.2. LVDT

LVDT (linear variable displacement transformer/linear variable displacement transducer) is a common type of transducer that converts the linear motion of a measured object into a corresponding electrical signal.

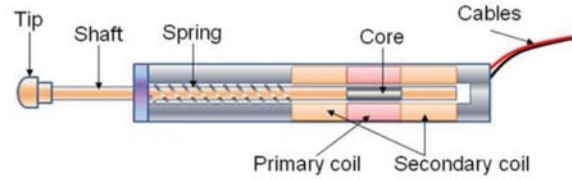


Figure 2. Parts of the LVDT [2]

The LVDT consists of a cylindrical tube that contains a measuring rod (Figure 2). The base of the tube is attached to a fixed position, and the end of the rod is attached to the moving object. The gauge does not touch the inside of the tube, making it virtually frictionless, and the LVDT's construction contains no electronic components, making it universally used in harsh measurement environments.

The LVDTs can measure movements as small as a few millionths of an inch to several inches but can also measure positions up to  $\pm 30$  inches ( $\pm 0.762$  meters). LVDT is an electronic device with both electrical and mechanical processes, needs an external power source to function, stores electromagnetic energy and converts some form of energy into a readable signal to describe the motion of an object along a single axis. The operating principle of the LVDT is depicted in Figure 3.

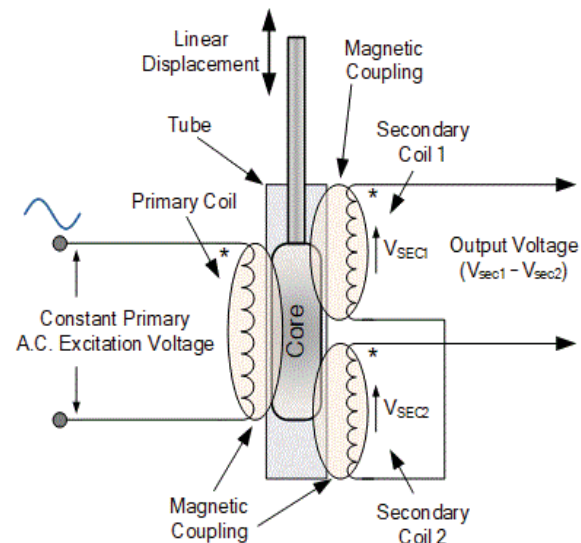


Figure 3. Working principle of LVDTs [3, 4]

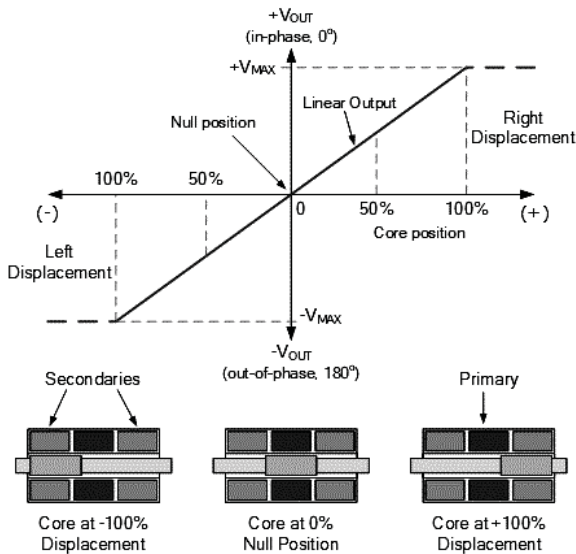


Figure 3 (tiếp). Working principle of LVDTs [3,4]

Unlike the Dial indicator, LVDT can eliminate almost all errors due to friction during measurement, tiny touching force, and high accuracy, making it applied in many geotechnical experiments. Some examples of using this classical surface settlement method were those of [5] and [6]. LVDT sensors are commonly used in measurement due to their high accuracy.

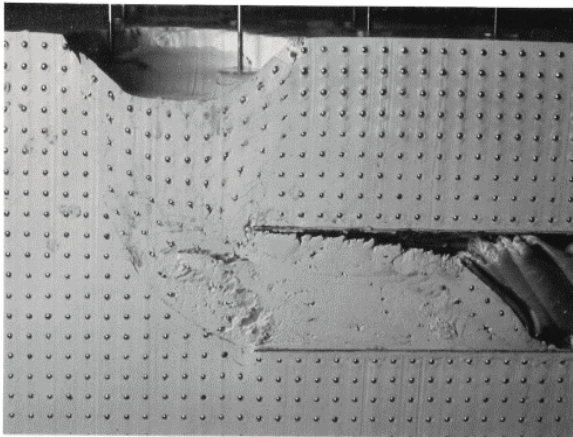


Figure 4. Observed surface settlement by LVDTs [6]

However, an undeniable disadvantage is that the number of measurement points will be limited and depend on the size of the experimental model, which is usually insignificant. The limited number of measuring points makes it challenging to reproduce displacement curves. In addition, it requires the experimenter to predict the critical locations to be measured before installation as in Figure 5. The measurement results will only show much information if this prediction is accurate.

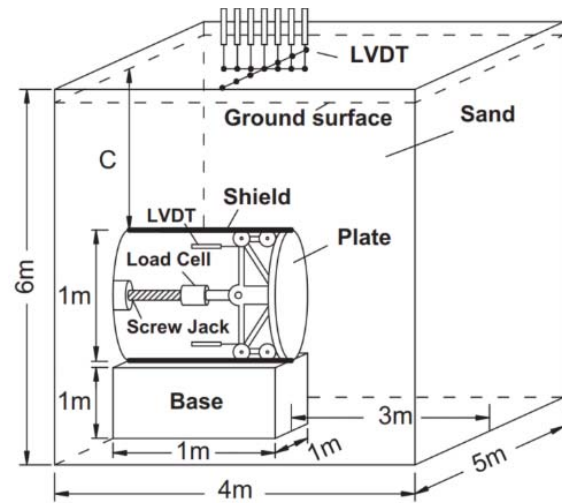


Figure 5. Setup of a tunnel model [5]

### 1.3. Laser camera

This type of equipments uses laser light to determine the distances. A typical laser camera is the LiDAR: Light Detection and Ranging is a device that uses infrared (IR). The type of laser camera, mentioned in this paper, is now a commercialized one and can easily purchase in Vietnam. The principle of this method is to measure the time it takes for a laser beam to be emitted from a photodiode, hit an object, and then reflect a detector. The distance will be calculated according to the speed and time of the light wave.

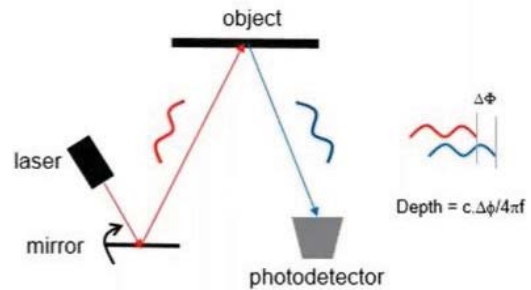


Figure 6. Working principle of the Lidar cameras [7]

This principle, called the time of flight (ToF), has been used in many distance measuring devices. However, such devices usually consist of only a fixed laser beam, which is directed towards the object. This principle causes such devices to measure the distances of points only sporadically. Unlike them, Lidar cameras integrate a Micro-Electro-Mechanical System (MEMS). This system consists of a micromirror that can change the inclination angle in two perpendicular directions thanks to electromagnetic forces. The laser beam will be beamed through the micromirror, then

reflect the object. Because the micromirror changes its angle continuously, the laser beam will be scanned across an area, not just fixed at a point. A receiver will record the laser beam reflected from the object, see Figure 6.



<b>Depth technology:</b> LIDAR	<b>Depth Field of View (FOV):</b> 70° × 55° (±3°)
<b>Minimum depth distance (Min-Z) at max resolution:</b> ~25 cm	<b>Depth output resolution:</b> Up to 1024 × 768
<b>Depth Accuracy:</b> ~5 mm to ~14 mm thru 9 m <sup>2</sup>	<b>Depth frame rate:</b> 30 fps

**Figure 7. The appearance and main features of the Lidar L515 [7]**

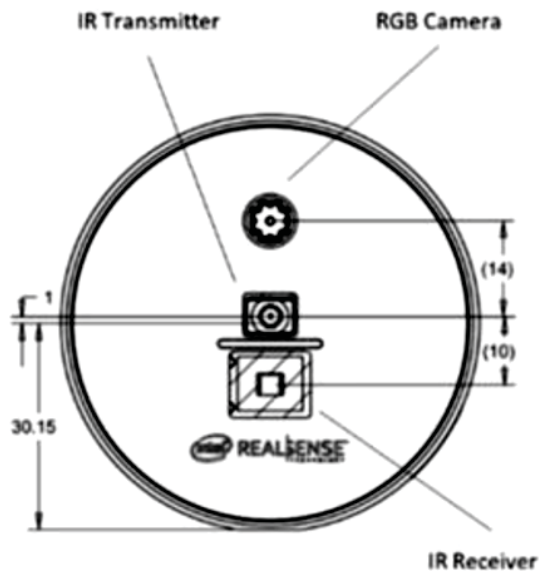


**Figure 8. Arrangement of transceivers on the front of LiDAR Camera L515 [7]**

Continuous-wave (CW) sensors measure the phase difference between the transmitted and received signals. The phase is calculated via demodulation. Depth estimation based on phase measurement suffers from an intrinsic phase-wrapping ambiguity. The microprocessor will then reconstruct the points (called point clouds) the laser beam has traveled to.

The appearance and main features of the Lidar L515 camera, which was used in the experiments of this article, are shown in the Figures 7 and 8.

Lidar L515 was applied to observe surface subsidence in a model experiment of tunneling in sandy soil. The experiment simulates the case of a collapsed tunnel in soft soil leading to subsidence at the surface.

## 2. TEST PROGRAM

### 2.1. Experiments setup

The test program includes the following stages:

- Conduct experiments to determine the parameters of the material (sand).

- Experiment with the model. The experimental setup is illustrated in Figure 9. The first step is to fabricate, install and calibrate the experimental equipment:

- The pistons were made and calibrated to ensure proper clearance (not so large that sand can pass through, nor so small that the pistons can get stuck).
- The position of the junction between the piston and the pull-out unit were put correct vertically and horizontally to ensure that the piston always moves parallel to the centre line of the tunnel.
- The normal camera recording movement below the surface (Sony camera) was placed far enough to limit the error due to the shooting angle (in this study, the distance is 1.5m, then the largest possible shooting angle is the case of cover thickness  $c = 25\text{cm}$ ; thus,  $\tan\theta = 25\text{cm}/150\text{cm} = 0.17$ ). The camera was adjusted so that its sensor position is at the same height as the tunnel's crown and the optical axis perpendicular to the wall of the container. This activity limited image distortion due to optical effects, which could lead to errors when measuring the image later.
- Depth measurement camera was placed about 40cm from the surface, ensuring greater than the minimum distance announced by the manufacturer (25cm) and achieving good resolution.
- Sufficient lighting and background arrangement for clear, uncluttered images by exterior details.
- Positions of the container and the pulling-out unit were fixed on a stable table with

wooden logs. These wooden logs were stuck on the table to keep the system exactly in the same position in all the tests of each test series.

- The test series were carried out for each type of sand with different cover thicknesses. The data were recorded and transferred to the computer for processing. The position of the test equipment was checked and calibrated correctly before each experiment.

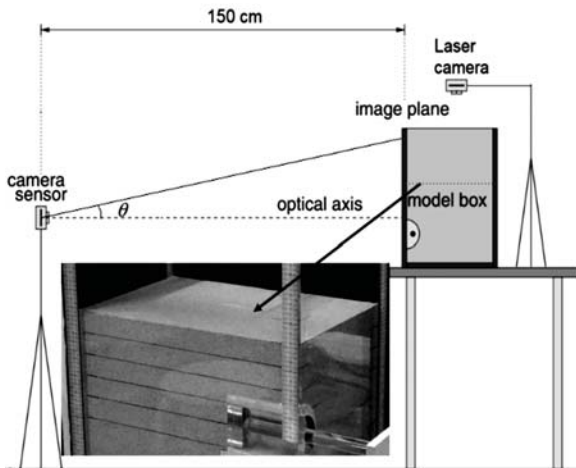


Figure 9. Set-up of the test/ Sand preparation for experimental model

## 2.2. Material properties

There were three types of sand are used: Toyoura, Silica Number 6 and silica number 5. Figure 10 shows the actual images of the sands. Toyoura is light yellow, Silica No. 5 and No. 6 are greys, but Silica No.5 has black particles. Toyoura sand is the finest type, and Silica No.5 is the coarsest. Index properties of sands is summarized in Table 1, in which friction angles were determined by direct shear tests.



Figure 10. Actual images of the three types of sand used in this study

Table 1. Index properties of sands

Index property	Toyo-ura	Silica No.6	Silica No.5
Specific gravity, $G_s$ ( $g/cm^3$ )	2.645	2.642	2.646
Mean grain size, $D_{50}$ (mm)	0.19	0.32	0.58
Effective grain size, $D_{10}$ (mm)	0.14	0.19	0.32
Uniformity coefficient, $U_c$	1.56	1.95	2.03
Friction angle, $\phi$ (degree)	34.8	37.7	36

The sand was carefully poured layer by layer into the box with a small shovel to prevent any compaction action. Each layer of 2.5cm in thickness (equal to half of the inner diameter of the tunnel) was levelled from the bottom of the tunnel and then sprinkled with a narrow colour sand band on the observation side. Before sprinkling the colour sand, testing sand on the observed side was levelled well by a ruler to ensure the creation of a very straight line of colour sand. The top layer was levelled thoroughly to adopt a good flat surface.

## 2.3. Setting up cameras

A laser camera for observing surface subsidence was set up on the top of the container. It was connected to a laptop to operate and capture images.

A regular camera, Sony DSC-WX500, with a resolution of 10 Megapixels (3,648 px × 2,736 px), was set up on the side of the model where it could observe the half tunnel. The camera was placed 1.5m from the container and at the same level as the tunnel. Sony camera was placed in the proper position, adjusted exposure rate and focus length to adopt good pictures. Lidar camera was connected to a laptop, set to the appropriate mode (short range) and start streaming. Figure 9 shows the experimental configuration after finishing preparation.

After the testing container and pulling-out unit were put in the right position, they would be fixed. The piston was attached to the pulling-out unit at the end of the rod. The face panel then was placed to the proper position (at the end of the tunnel).

After finishing the preparation, the experiments were performed. The piston was pulled out at particular stops. At every stop, soil movements were captured on both sides (from the top side by the Lidar camera and the lateral side by the Sony camera). The initial position is point zero; next stops increase distances to the initial stop. The list of stops is as follows: 1, 2, 3, 4, 5, 6, 8, 10, 12, 14,

18, 21, 24, 27, 30, 33, 36, 40, 44, 48, 52, 56, 60, 65, 65+ 5, ...X mm.

Where X is the maximum pull-out length, the position where the toe of the sand dune stops developing. All the results in this article were the cases of X values.

The tests were performed with three dry sand types for various  $c/D$  ratios, where  $c$  is the thickness of sand above the tunnel;  $D$  is the inner diameter of the tunnel. The cases of experiments are summarized in Table 2.

**Table 2. Nine cases of the experiment**

c/D	Toyoura	Silica No.5	Silica No.6
1	√	√	√
1.5	√	√	√
2	√	√	√

#### 2.4. Data and analysis

Data were read and recorded by software of Intel named Intel RealSense™ LiDAR Camera L515. After every step of the process, live streams were paused to export data to a \*.PLY file. The data were a collection of points (point clouds) representing 3-dimensional distances to the camera sensor. This set of points forms a surface that the laser beams across during the capture. The recorded data were then analyzed by an open-source software called CloudCompare V.2.

This software allows manipulating the point cloud directly as a specific object while preserving their shape and size as they were recorded. Users can measure the distance between any two points; distance data is shown in 3 axes x, y, and z, see Figure 11. In the scope of this study, the features of CloudCompare are sufficient to perform the necessary analysis.

The sequence of data processing is as follows:

- Open data file \*.PLY with *CloudCompare software*.
- Cut out the excess, keep only the surface image data of the model.
- Rotate the point cloud to the standard position (corresponding edges are parallel to the  $x$ ,  $y$ , and  $z$  axes).
- Change the color display mode (scalar field) according to the depth parameter ( $z$ -axis).
- Save the data file with the corresponding name, the file after processing will be in \*.BIN format.
- Take pictures of the background model surface of the cases to compare with each other.
- Define necessary geometry parameters and write to excel data file.
- Repeat with all cases to obtain the geometry dataset.
- Processing geometric data sets using *Microsoft excel software*.

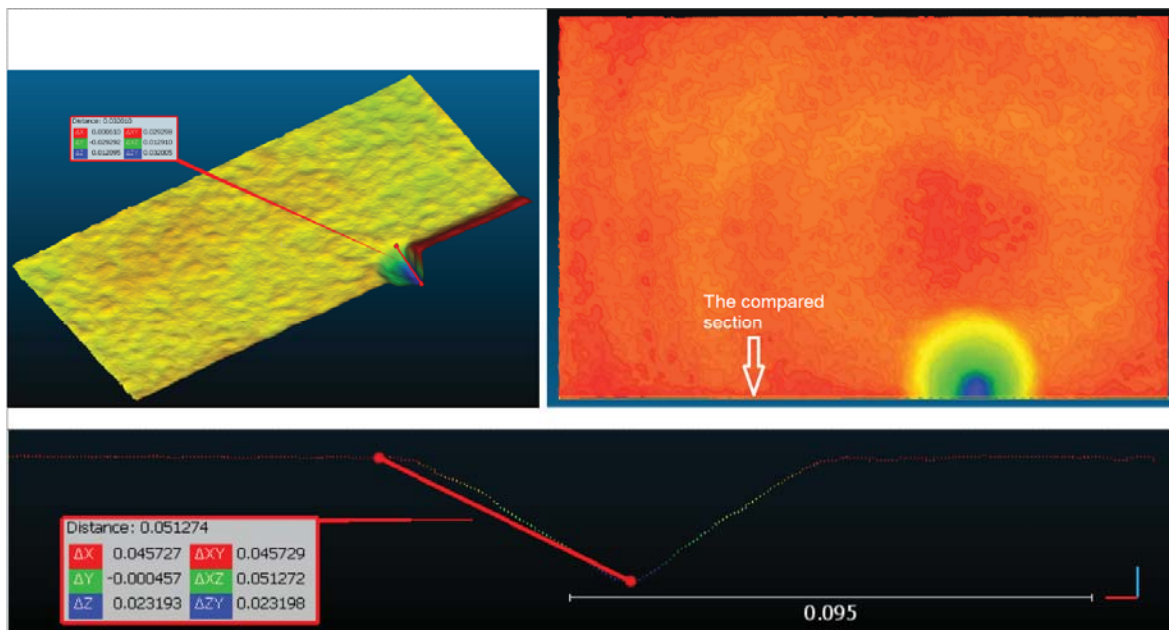


**Figure 11. Example of defining information geometries using CloudCompare**

Use the Cloud Compare software to separate a narrow strip (about 1-1.5mm) at a position close to the front wall of the test box, which is the position captured by a regular camera. This narrow band is a minor point cloud; their coordinates are exported to Excel for further processing as follows:

- Draw a graph of the coordinates of the points vertically and horizontally (at each position, there will be a certain number of points depending on the width of the narrow strip cut before)

- Bring the chart to a position with convenient coordinates for analysis (average points at the surface are brought back to coincide with the  $z=0$  line, the first point is horizontally located at coordinates (0,0)). The plot of the coordinates of the points is placed together with the image taken with the regular camera for comparison (Figure 12).

### 3. RESULTS AND DISCUSSION

According to the manufacturer, the depth error average at 1m distance from the camera is  $<5\text{mm}$  at 95% reflectivity. The depth measurement error announced by the manufacturer is 5mm to 14mm through a measuring range of  $9\text{m}^2$ , equivalent to a distance of 2,485m. Thus the error ranges from 0.2% to 0.56%. Manufacturer also recommended that the images taken with the lidar camera are placed in short-range mode would obtain higher accuracy [7]. The actual experimental distance of about 40cm. Captured images were analyzed to check the tolerance of the device. The comparison was made at the side of the test container, where the data were recorded by both the ordinary camera and the lidar camera, Figure 13. On this cross-section, the sinkhole's depth data ( $\Delta z$ ) was measured by the CloudCompare software and directly on the image taken with the ordinary camera. The difference between the results obtained from the laser camera (Lidar L515) and the camera is summarized through the graph in Figure 12.

The measurement results in the experiment had an average error of 1.68mm with a measuring range of 40cm, equivalent to an error of 0.42%, consistent with the manufacturer's announcement.

The graph shows that the values measured by the camera laser are all smaller than those measured directly by conventional optical principles; the average difference is 8.86%. The deviation did not show a relationship with the grain size of the sands used. This deviation is difficult to meet the requirements of standard model testing. Therefore,

direct use of depth measurement results from Lidar L515 is not recommended for model testing.

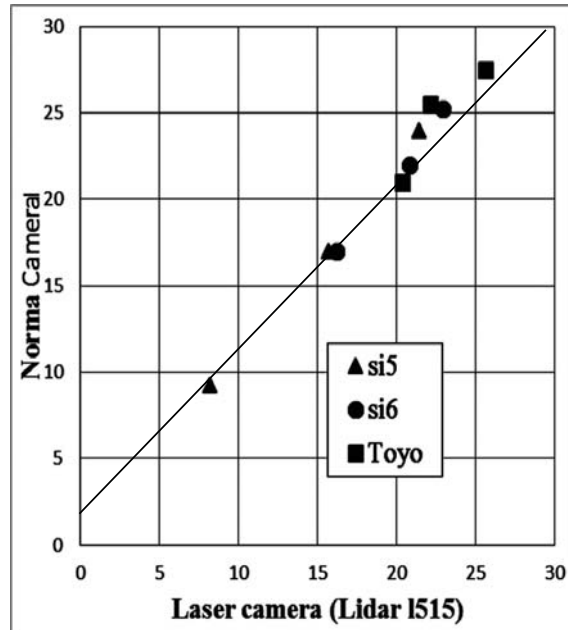


Figure 12. Measured values from 2 types of cameras (mm)

The horizontal accuracy was not measured, but the observation in Figure 13 showed a very high similarity in the settlement curve shape in the survey section. The similarity is shown consistently across all nine survey cases. Ground observations are also carried out. The 3d images taken from the Lidar camera are taken according to the plan view; these images are compared with those taken with the regular camera, combined with lighting effects to see the subsidence area (Figure 14). The similarity in shape is easily seen in the comparison figures

The above observations show that the absolute depth measurement value from the lidar camera is not accurate enough for the experimental requirements. However, the error ratio of the measurement points in the settlement area is uniform, so the overall shape of the area subsidence is still guaranteed. This feature can be used to overcome the disadvantage of data discretization when using LVDT. How to proceed as follows:

- Using laser camera and ordinary camera to track vertical displacement of the ground surface in the way applied in the experiment in this paper;

- Use one or more LVDTs to measure the vertical displacement of the surface at the section close to the section observed by conventional cameras.

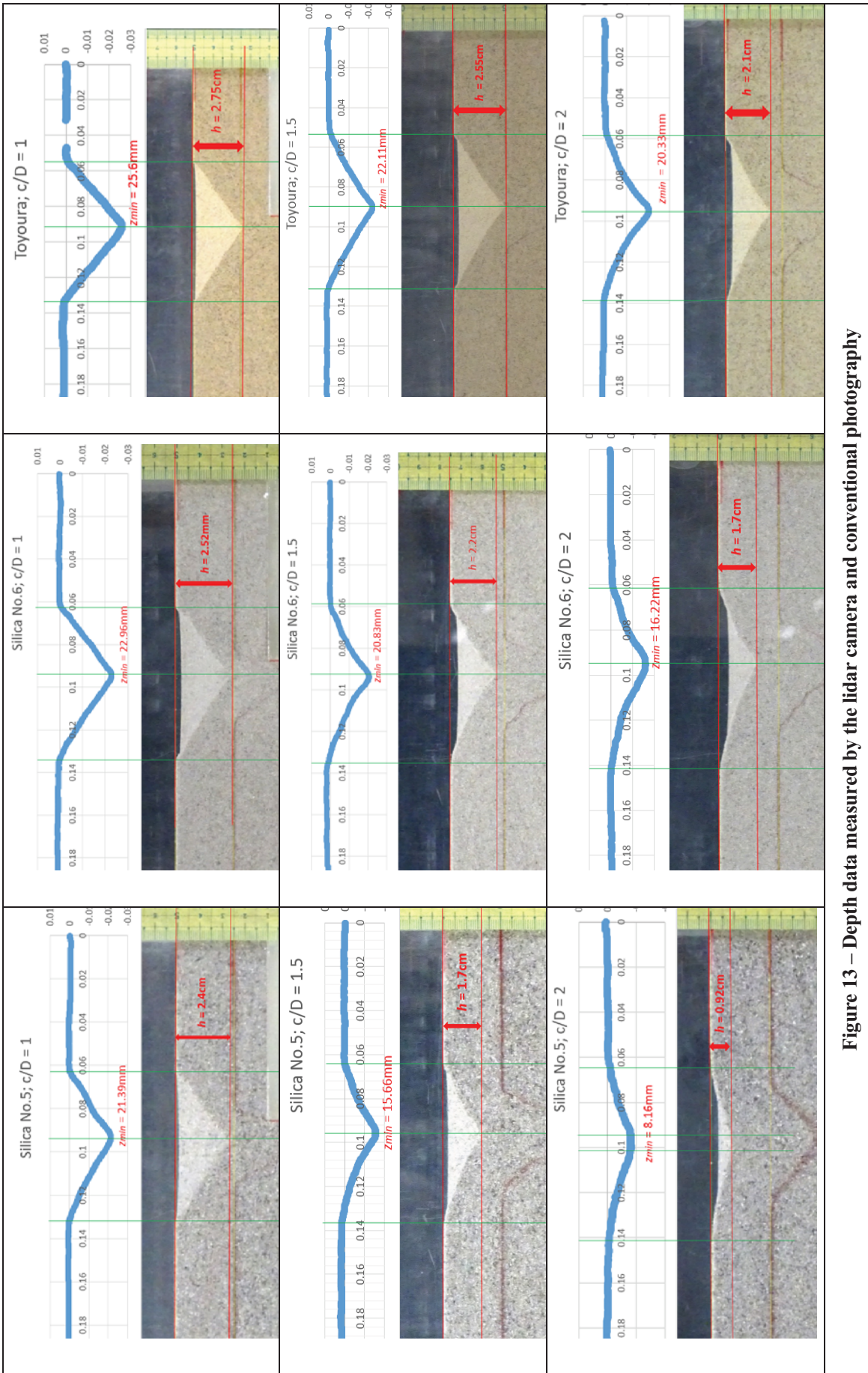


Figure 13 – Depth data measured by the lidar camera and conventional photography



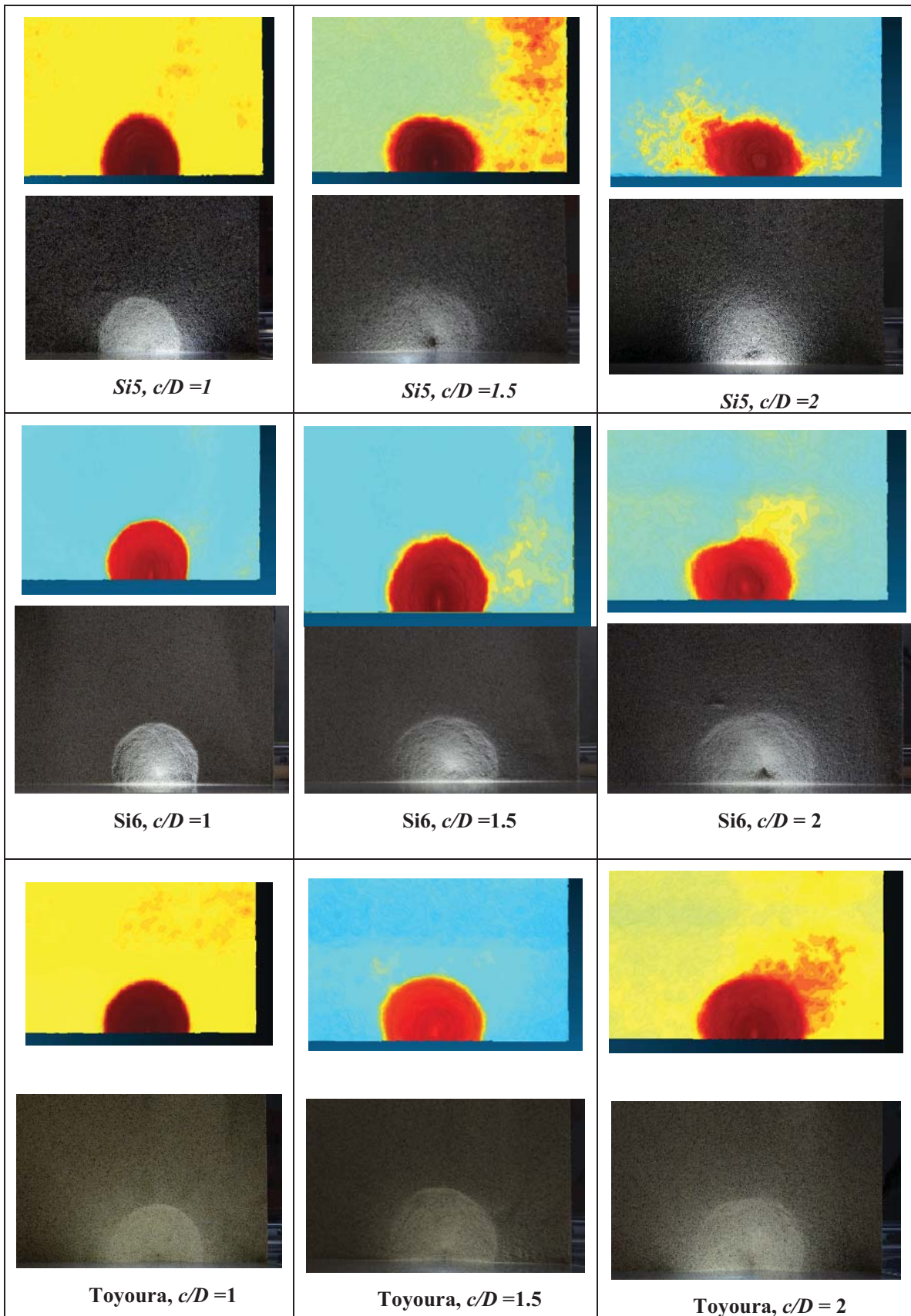


Figure 14 - Surface images comparison between the Laser camera and the normal camera

- The measured data where the LVDT is placed are extracted for analysis. In which the measured value of LVDT is taken as the standard, the measured value at that location from the camera lidar is used for comparison. From there, the error coefficient of the lidar camera can be established for the experimental cases.

- The deviation coefficient is used to calculate all positions in the settlement area from the data of the Lidar camera for the experimental cases.

#### 4. CONCLUSION

- LVDT is a reliable and commonly used device for displacement measurement, but it only measures a finite number of discrete points, making it difficult to reconstruct a whole surface.

- Easy-to-use lidar camera L515 allows measuring a large set of points quickly, but the error in distance measurement results by a lidar camera is difficult to meet the accuracy requirements in model experiments.

- Combining two measurements can help to overcome the disadvantages mentioned above; a procedure has been proposed to combine these two measurements to achieve the required accuracy and

allowability of a set of points large enough to represent the displacement surface.

#### REFERENCES

- [1] <https://th.misumi-ec.com/en/vona2/detail/223006556199/>
- [2] <https://www.electronics-tutorials.ws/io/linear-variable-differential-transformer.html>
- [3] <https://www.te.com/usa-en/products/sensors/position-sensors/intersection/lvdt-tutorial.html>
- [4] <https://learnmech.com/what-is-lvdt-diagram-advantages-and-disadvantages/>
- [5] Chen, R.P., Li, J., Kong, L.G., Tang, L.J., (2013). *Experimental study on face instability of shield tunnel in sand*. Tunnel. Undergr. Space Technol. 33, 12–21.
- [6] Mair, R.J., (1979). *Centrifugal Modelling of Tunnel Construction in Soft Clay*. Ph.D. thesis, University of Cambridge, Cambridge, U.K.
- [7] <https://www.intelrealsense.com/lidar-camera-l515/>.